Journal of Thermal Analysis, Vol. 35 (1989) 2199–2212

CHARACTERIZATION AND THERMOANALYTICAL INVESTIGATIONS OF SILVER TELLURITE

*I. B. Sharma** and *S. Batra*

DEPARTMENT OF CHEMISTRY, UNIVERSITY OF JAMMU,
JAMMU TAWI–180004, INDIA

(Received May 16, 1988; in revised form November 16, 1988)

Silver tellurite, prepared by precipitation, crystallized in tetragonal form and DSC studies show that it undergoes phase transformations on heat-treatment in the temperatuae ranges 578–604 K and 695–717 K. X-ray diffractometry suggests that in the first transformation, which is irreversible, the tellurite transforms to monoclinic form. The second transformation is reversible and the high temperature phase reverts back to the monoclinic form on cooling. The reversible phase transformation could be ascertained by electrical resistivity and reflectance spectrum measurements. The kinetic parameters, computed from the DSC data, show that the energy of activation, entropy of activation and the frequency factor are high. This is attributed to the effectiveness of a large number of vibrations.

Numerous tellurites have been described in the literature and these have been studied to understand their structure and other related properties [1–5]. Investigations on silver tellurite, prepared by precipitation, show that it undergoes phase transformations on heat-treatment [3]. However, there appear to be no papers on the characterisation of the phases formed and on the mechanism of these transformations. In the present investigation, silver tellurite, prepared by precipitation, has been subjected to thermogravimetric and differential scanning calorimetric analysis to ascertain thermal effects. Different phases have been identified by X-ray diffractometry and chemical analysis. Magnetic susceptibility and electrical resistivity, as functions of temperature, and room temperature reflectance spectra have been recorded to gain further information. From the thermal data, kinetic parameters have been computed.

* To whom all correspondence should be addressed.

John Wiley & Sons, Limited, Chichester
Akadémiai Kiadó, Budapest

Experimental

Preparation of silver tellurite

AR grade silver nitrate, sodium carbonate and tellurium dioxide were used as starting materials. Silver tellurite was prepared by slow addition of an aqueous solution of silver nitrate to a solution of sodium tellurite at 303 K. The yellowish white precipitates were washed with distilled water and dried in vacuum at 353 K. To further dry and stabilize the sample, it was heated at 523 K for six hours in static air atmosphere. Sodium tellurite required for this purpose was prepared by the usual method of fusion of sodium carbonate and tellurium dioxide in equimolar proportion at 1070 K [3]. The composition of the tellurite was determined by elemental analysis using accepted methods [6].

Thermal analysis

The sample was thermally analysed by a Mettler TA–3000 thermal analysis system, provided with microprocessor TC–10, for differential scanning calorimetric and thermogravimetric studies in the temperature range 313–733 K at the heating rates of 5.7 and 10 deg/min in air atmosphere. The cooling curves of the samples were also recorded at a cooling rate of 10 deg/min. The DSC and TG–DTG curves

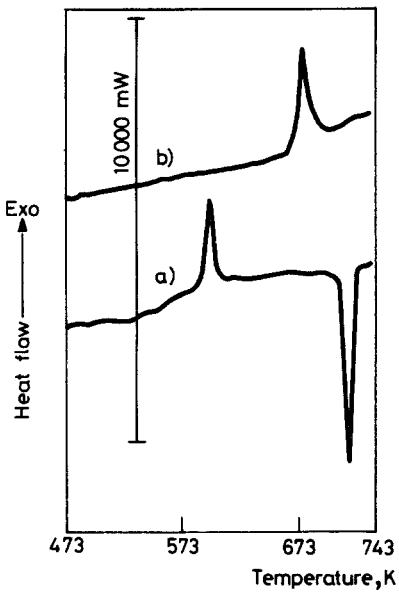

Fig. 1 (a) DSC curve (dH/dt *vs.* T) for silver tellurite at a heating rate of 10 deg/min. (b) Cooling curve at a cooling rate of 10 deg/min. Sample wt.: 20.781 mg

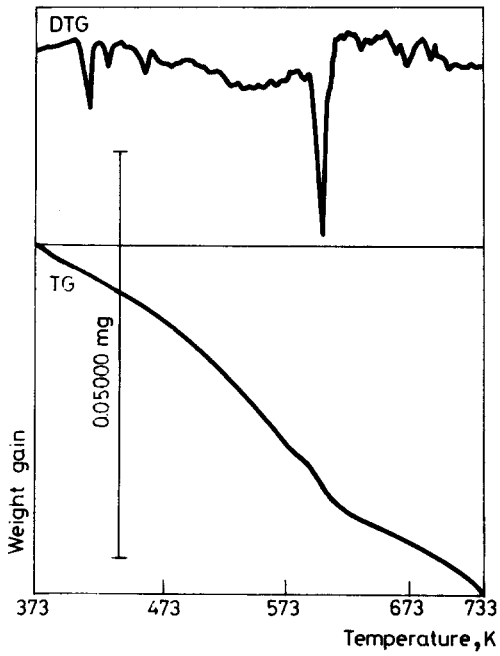

Fig. 2 TG–DTG curves for silver tellurite at a heating rate of 10 deg/min. Sample wt.: 7.530 mg

recorded at a heating rate of 10 deg/min are given in Figs 1 and 2. The C_p *vs.* T curve in the temperature range 633–733 K (Fig. 3) was computed with reference to the blank curve, using the base line type 11. The reversibility of the transformation and the effect of repeated heating was further ascertained by cooling the sample to room temperature after recording DSC curves upto 717 K, and rerun at the same heating rate.

To confirm that the tellurite does not melt up to 733, the sample was heated on a locally fabricated hot-stage and observed under a metallurgical microscope.

X-ray diffractometry

Room temperature X-ray powder patterns of the silver tellurite and the samples taken from the DSC cell after runs up to 626 K and 717 K and the sample quenched in water, after heat-treatment up to 717 K, were recorded by Phillips diffractometer type PW 1050/70 at a scanning speed of 1 deg/min. The radiation used was CuK_α (λ = 1.7902 Å). The diffractograms of the first three samples are given in Fig. 4. The data were indexed for determination of cell parameters and the parameters were refined by computer programme [7]. The experimental and calculated X-ray diffraction data are given in Tables 1–4.

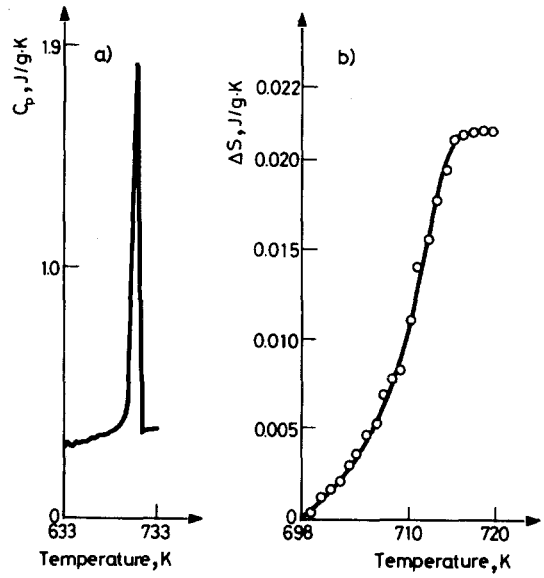

Fig. 3 (a) Plot of C_p *vs.* T for the phase transformation in the temperature range 695–717 K. (b) ΔS *vs.* T curve for the transformation

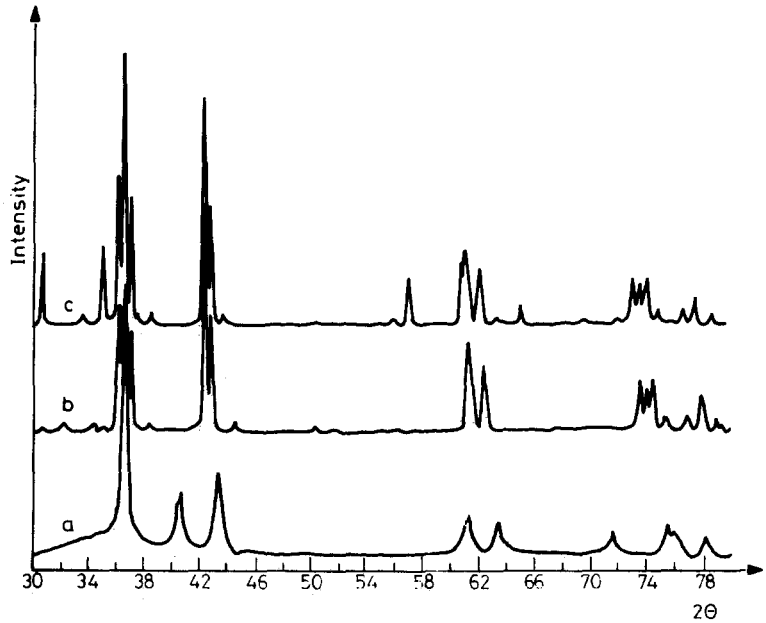

Fig. 4 X-ray diffractograms of (a) silver tellurite, (b) the sample pre-heated at 626 K and (c) the sample pre-heated at 717 K

Table 1 X-ray powder diffraction data for silver tellurite

hkl	I/I_0	d_{exp}, Å	d_{cal}, Å (±0.003)
112	100	2.853	2.846
220	23	2.580	2.563
300	32	2.419	2.417
401	16	1.753	1.752
411	10	1.699	1.703
332	8	1.530	1.529
422	11	1.463	1.465
431	7	1.419	1.419

Unit cell parameters: $a = 7.250 \pm 0.124$; and $c = 6.843 \pm 0.118$ Å

Table 2 X-ray powder diffraction data for silver tellurite heat-treated at 717 K

d_{exp}, Å	I/I_0
3.403	24
3.101	5
2.981	28
2.885	53
2.858	100
2.817	43
2.788	3
2.722	5
2.481	82
2.456	42
2.402	4
1.900	3
1.873	17
1.761	23
1.757	27
1.730	20
1.701	3
1.661	7
1.501	16
1.493	7
1.484	14
1.470	3
1.444	4
1.429	9
1.409	4

Table 3 X-ray powder diffraction data for silver tellurite quenched after heat treatment at 717 K

d_{exp}, Å	I/I_0
2.884	54
2.858	100
2.816	52
2.722	8
2.478	93
2.451	87
1.759	28
1.729	27
1.501	20
1.491	3
1.485	16
1.471	5
1.445	4
1.430	9
1.410	4

Table 4 X-ray powder diffraction data for silver tellurite heat-treated at 626 K

d_{exp}, Å	I/I_0
3.403	2
3.228	4
3.036	4
2.885	54
2.858	100
2.817	43
2.722	6
2.481	99
2.456	50
2.361	4
1.761	36
1.730	25
1.501	22
1.493	9
1.484	19
1.467	6
1.439	6
1.425	13
1.407	4

Magnetic susceptibility and electrical resistivity

Magnetic susceptibility was recorded by a Gouy magnetic balance, keeping the field strength constant at 3000 gauss for all measurements. $HgCo(CNS)_4$ was used as calibrant. The electrical resistivity of pellets of silver tellurite, sintered at 717 K for 24 hours, was measured as a function of temperature by the two-probe method. The sintered pellets were held tightly in between two platinum plates and the resistance was measured directly by a $4\frac{1}{2}$ digit ECIL digital multimeter. The measured resistance, R, was converted to specific resistance, using the dimensions of the pellets. A plot of $\ln \varrho$ versus $1/T$ is given in Fig. 5.

Reflectance spectra

Reflectance spectra of the samples were recorded in the range 2500–250 nm by a DM R2 spectrometer. The plots are given in Fig. 6.

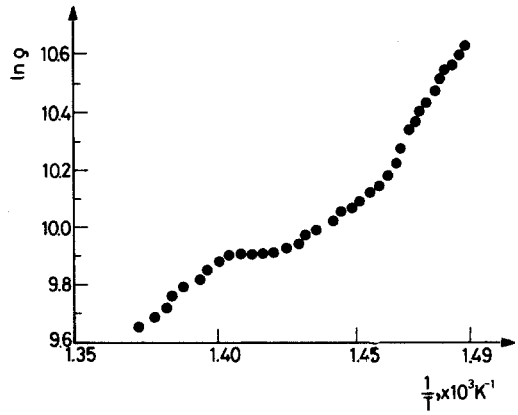

Fig. 5 Plot of $\ln \varrho$ versus $1/T$

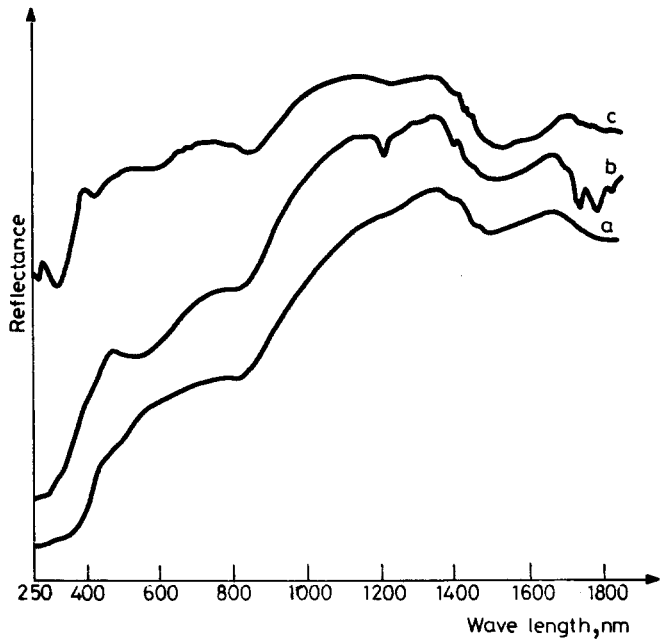

Fig. 6 Reflectance spectra of (a) silver tellurite, (b) the sample pre-heated at 626 K and (c) the sample pre-heated at 717 K

Macrophotographs

Macrophotographs of the precipitated silver tellurite and the sample, pre-heated at 717 K, have been taken using a Carl Zeiss inverted type metallurgical microscope attached with a dark field illuminator (Neophot–2). The macrographs are given in Fig. 7.

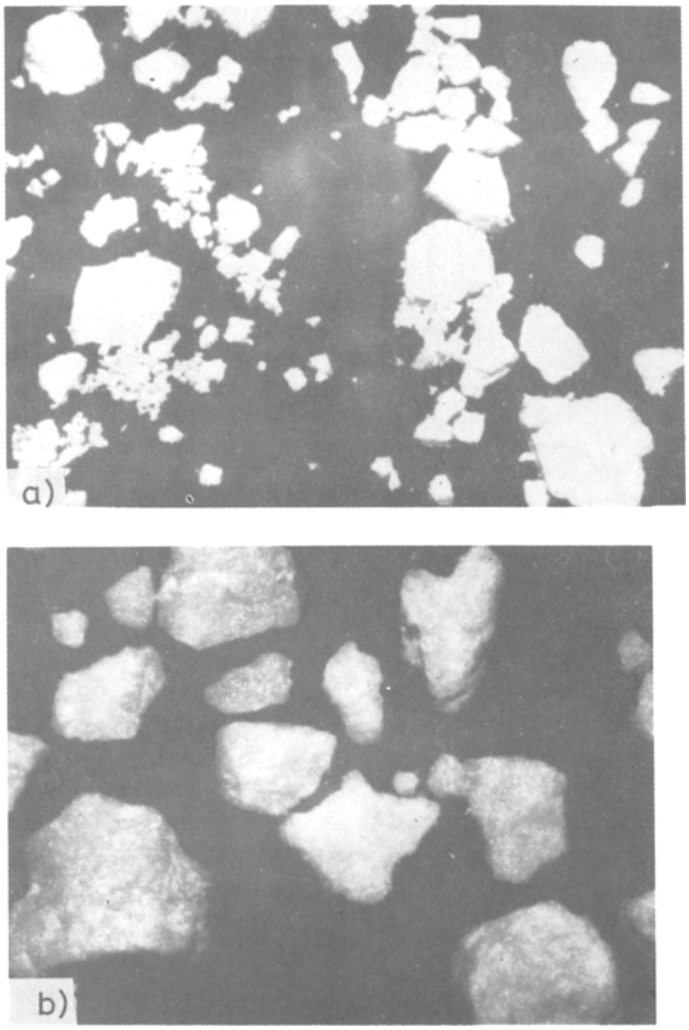

Fig. 7 Macrographs of (a) silver tellurite (×40) and (b) the sample pre-heated at 717 K (×40)

Results and discussion

Chemical analysis of silver tellurite suggested that Ag and Te were present in 55.4% and 32.3%, respectively. By difference, 12.3% oxygen is present. This suggests the stoichiometry of the sample as $Ag_2Te_{0.99}O_{2.88}$. For the sample taken from the DSC cell after a run up to 717 K, elemental analysis shows that Ag and Te percentage was equal to 55.8 and 32.0 respectively, which suggests its stoichiometry as $Ag_2Te_{0.97}O_{2.94}$. The minor change in stoichiometry from $Ag_2Te_{0.99}O_{2.98}$ to $Ag_2Te_{0.97}O_{2.94}$ is attributed to the general tendency of tellurium compounds to lose tellurium on heat-treatment. In the present case, the heat-treatment of the material results in the minor loss of tellurium and the corresponding oxygen content.

The differential scanning calorimetric curve of silver tellurite (Fig. 1a) shows two transitions. The first transition, lying between 578 K and 604 K with peak temperature at 592.6 K, is exothermic, while, the second transition, lying between 695 K and 717 K with peak temperature at 713.2 K, is endothermic. The cooling and rerun curves for the sample show that the first exothermic transition is irreversible, while the endothermic transition is reversible. The shift in peak temperature (38.6 K) observed in the cooling curve (Fig. 1b) is due to thermal hysteresis, which is a necessary consequence of co-existence of the two phases over a range of temperature. Generally, phase transformations are endothermic, while the first transformation in the present study is exothermic. This is because of the fact that tetragonal silver tellurite, which is metastable, transforms to a more stable and low energy orthorhombic phase, resulting in the exothermic process.

The TG–DTG curves (Fig. 2) suggest a continuous mass loss during heat-treatment. The loss is 0.7% at 717 K. This mass loss is in accordance with the stoichiometric change from $Ag_2Te_{0.99}O_{2.98}$ to $Ag_2Te_{0.97}O_{2.94}$, as suggested by the elemental analysis. The re-run TG–DTG studies show that the tellurite continues to lose mass, although without any pronounced fall. The re-run DSC curve for the sample shows that enthalpy change associated with the reversible transformation is almost three times the enthalpy value for the transition in the freshly precipitated sample. The nature of a peak in a solid state transition is known to depend very strongly on the pre-treatment of the material [8]. In the present case, it is attributed to an increase in particle size and disappearance of dislocations and grain boundaries on heat-treatment. Macrographs of the sample before and after heat-treatment amply substantiate that the particle size increased on heating, while the fresh sample was an aggregate of tiny particles (Fig. 7).

The X-ray diffraction pattern of the precipitated sample (Fig. 4 and Table 1) could be indexed on the basis of a tetragonal unit cell with $a = 7.250$ and $c = 6.843$ Å, while the data for the sample heated up to 626 K have been indexed

for monoclinic unit cell with $a = 7.00$, $b = 10.509$ and $c = 4.911$ Å and $\beta = 91.50°$. The unit cell dimensions determined from our experimental data for the heat-treated sample are in agreement with those reported by Masse et al. for the high temperature phase [9]. Some additional lines have been observed in the present case, which, of course, could be indexed according to the monoclinic unit cell dimensions. The data for the other two samples, one prepared by slow cooling and the other by quenching the sample after heat-treatment up to 717 K also have been indexed for the monoclinic unit cell.

In order to gain information on the crystallite size, full half-widths from the X-ray peaks for highly crystalline silicon sample and those for the silver tellurite samples have been calculated (Table 5). These results suggest that the crystallite size for the tetragonal sample is small. The slowly cooled as well as quenched samples, after heat-treatment up to 717 K, are better crystallized than the sample heated up to 626 K.

Table 5 The half widths from X-ray diffractograms of highly crystalline silicon and the tellurite samples

Sample	*hkl*	$W_{1/2}$ (in degree 2θ value)
Silicon	111	0.17
Silver tellurite	112	0.40
dried at 523 K	220	0.25
	300	0.43
Silver tellurite	021	0.26
heat-treated at 626 K	003	0.23
	114	0.35
Silver tellurite	021	0.18
heat-treated at 717 K	003	0.21
(slowly cooled)	114	0.30
Silver tellurite	021	0.20
heat-treated at 717 K	003	0.22
(quenched)	114	0.28

The X-ray diffraction data when analysed in the light of DSC results show that silver tellurite precipitates in tetragonal form and transforms to the monoclinic form in the temperature range 578–604 K. The transformation process is irreversible. According to Buerger's classification, in this case a change in primary coordination takes place which involves making and breaking of bonds and should be associated with high activation energy [10]. This is substantiated by the energy of activation computed for the transition (Table 4), which is as high as 1295 kJ/mol. The DSC curve shows that the sample undergoes another phase transformation in

the temperature range 695–717 K, which is reversible. The room temperature X-ray diffraction data of the sample, obtained after the transition, show that the sample is reverted back to the monoclinic form, the crystal structure in which it existed before the transition. The only difference that arises is a change in intensity of certain lines and some additional peaks, which of course could be fitted into the same unit cell. The change in intensity and the additional peaks are attributed to a higher perfection achieved by the crystal structure. As there is not much difference in the structures of the slowly cooled and quenched samples, after heat-treatment up to 717 K, and the hot stage microscopic study shows that the sample remains in solid state in this temperature range, it may be assumed that the low temperature phase is a super-structure of the one which exists after the transition at 717 K.

Silver tellurite exhibits temperature independent weak paramagnetic susceptibility ($\sim 10 \times 10^{-6}$ cgs units mol^{-1}) in the temperature range 323–733 K, after diamagnetic correction for the constituent ions. This is expected as none of the constituent ions have any unpaired electron which could contribute to magnetic paramagnetism. The small paramagnetism is attributed to the collective behaviour of the electrons [11].

The electrical resistivity in the temperature range 670–730 K shows that the complex oxide is semiconductor in nature and exhibits anomaly at 712 K, which corresponds to the reversible phase transformation process exhibited by the DSC curve. From the $\ln \varrho$ versus $1/T$ plot (Fig. 5) the energy of activation for the electrical conduction before the transition is ~ 1.12 eV, while it is ~ 1.37 eV after the transition. Prediction of band formation is possible only when the complete crystal structure is known. However, because only a small change in the energy of activation for electrical conduction is associated with transformation, no change in the scheme of band formation seems to occur.

The room temperature reflectance spectra of the samples heat-treated at 626 K and 717 K (Fig. 6b, c) are similar in nature and show additional bands around 418, 600 and 1190 nm, as compared to the spectra for the sample before the heat treatment (Fig. 6a). The similarity in spectra (b and c) is expected because the process involved between these temperature limits is reversible. However, their difference from the spectra of the sample before heat treatment, which has quite different crystal structure, is very clear because of the additional bands in the spectra of the heat-treated samples.

Kinetics of phase transformations

Almost every kinetic method used in DSC is based on the equation [12, 13]

$$\frac{d\alpha}{dt} = Ae^{-E/RT}(1-\alpha)^n \qquad (1)$$

Assuming that the rate of the reaction is proportional to the DSC signal, the above equation in the logarithmic form is transformed to the following relationship:

$$\ln \frac{dH/dt}{H_t} = \ln A - \frac{E}{RT} + n \ln H_r/H_t \quad (2)$$

Where dH/dt is the rate of heat flow, H_t is the total enthalpy of the reaction and H_r is the difference between the total enthalpy (H_t) and the enthalpy change occurring for any fraction of the reaction (H_p).

From the DSC measurements dH/dt, H_t, H_r and T are known and the rest of the parameters can be calculated. On the basis of this principle n, A and E for the two transitions, exhibited by the differential scanning calorimetric study, have been calculated with the aid of programmes available with the microprocessor TC–10, provided with the thermal analysis system. The values of the parameters n, A and E are given in Table 6. The 95% confidence limits are large, suggesting higher uncertainty in these values. Because of the narrow range of transition temperature, $\ln A$ and E are very strongly correlated resulting in a higher degree of uncertainty in the kinetic parameters.

Table 6 Kinetic parameters (with 95% confidence limit in parentheses) for phase transformations in silver tellurite at a heating rate of 10 deg/min

Peak region, K	n	E, kJ/mol	$\ln A$	ΔH, J/g
578–604	1.34	1295	232	5.22
	(0.15)	(79)	(16)	
695–717	0.03	960	159	9.08
	(0.01)	(62)	(11)	
699–717	0.03	865	142	25.7
(pre-heated at	(0.02)	(58)	(10)	
717 K and re-run)				

The frequency factor for both transformations is far greater than the normal value predicted by the absolute rate theory. These values suggest that the partition function for the activated complex and the entropy of activation must be high. Applying the relation [14]

$$\Delta S^* = \frac{\Delta H^*}{T} + R \ln Kh/kT \quad (3)$$

where ΔH^* (for a solid state process) $= E - RT$. ΔS^* for the two transitions comes out to be 1.87 kJ K^{-1} mol^{-1} and 967 JK^{-1} mol^{-1} respectively. The unusually

high values of ΔS^* support the argument that the activated state is highly disordered and the partition function for this state must be very high.

The C_p *vs.* T curve for the phase transformation in the temperature range 695–717 K (Fig. 3) exhibits a sharp discontinuity at the transition temperature, while ΔS (calculated from the relation, $\Delta S = \int_{T_1}^{T_2} C_p \, \mathrm{d} \ln T$) *vs.* T curve shows no such sharp discontinuity. Thermodynamically, this is a continuous or second order transformation [15]. The transformation is associated with thermal hysteresis of 38.6 K, a phenomenon generally observed in reversible continuous transformations. The occurrence of thermal hysteresis shows that equilibrium is not complete at all the stages of the transformation as required by thermodynamics and the two phases co-exist over a range of temperature. From the fact that the order of reaction in this transformation is approaching zero, it may be concluded that the nucleation is initiated homogeneously throughout the bulk of the crystals resulting in a constant reaction rate during the transformation.

* * *

The authors are thankful to the University Grants Commission, New Delhi for the financial assistance. Thanks are also due to Professor K. N. Goswami for help in computer programming.

References

1 E. S. Ganelina and T. N. Pozhideava, Zh. Prikl. Khim., 38 (1965) 2210.
2 J. A. Alonso, A. Castro, A. Jerez, C. Pico and M. L. Velga, J. Chem. Soc. Dalton, (1985) 2225.
3 J. W. Mellor, A Comprehensive Treatise in Inorganic and Theoretical Chemistry, Vol. 11, Longmans, London, 1948, p. 77.
4 G. G. Gospondinov and B. G. Bogdanov, Thermochim. Acta, 77 (1983) 387.
5 O. Lindqvist, Acta Chem. Scand., 26 (1972) 1423.
6 A. I. Vogel, "Quantitative Inorganic Chemistry", Longmans, London, 1961.
7 R. Sharma, "M. Phil Dissertation", Jammu University, Jammu, 1985.
8 P. D. Garn, Analytical Calorimetry, Vol. 3, edited by R. S. Porter and J. F. Johnson, Plenum, New York, 1974, p. 787.
9 R. Masse, J. C. Guitel and I. Tordjman, Mat. Res. Bull., 15 (1980) 431.
10 M. J. Buerger, Soviet Phys. Cryst., 16 (1972) 959.
11 J. B. Goodenough, J. Appl. Phys., 37 (1966) 1415.
12 W. W. Wendlandt, Thermal Methods of Analysis, Wiley, New York, 1974, p. 187.
13 P. Peyser and W. D. Bascom, Analytical Calorimetry, Vol. 3, edited by R. S. Porter and J. F. Johnson, Plenum, New York, 1974, p. 537.
14 K. J. Laidler, Chemical Kinetics, Tata–McGraw Hill, New Delhi, 1983.
15 C. N. R. Rao, Modern Aspects of Solid State Chemistry, Plenum, New York, 1970, p. 589.

Zusammenfassung — Durch Ausfällen hergestelltes Silbertellurit kristallisiert tetragonal und DSC-Untersuchungen zeigen, daß es bei Einwirken von Wärme in den Temperaturbereichen 578–604 K und 695–717 K Phasenumwandlungen vollzieht. Röntgendiffraktometrische Untersuchungen lassen vermuten, daß sich das Tellurit bei der ersten Phasenumwandlung, die eine irreversible ist, in die monokline Form umwandelt. Die zweite Umwandlung ist umkehrbar und die Phase bei höherer Temperatur wandelt sich bei Abkühlen wieder in die monokline Form um. Die reversible Phasenumwandlung konnte mittels Messung des elektrischen Widerstandes und durch Aufnahme des Reflexionsspektrums festgestellt werden. Die aus den DSC-Daten berechneten kinetischen Parameter zeigen eine hohe Aktivierungsenergie, eine hohe Aktivierungsentropie und einen großen Frequenzfaktor. Dies wird der Wirksamkeit der großen Anzahl an Schwingungen zugeschrieben.

Резюме — ДСК исследования теллурита серебра показали, что он подвергается фазовым превращениям в области температур 578–604 К и 695–717 К. Рентгенофазовый анализ показал, что первое фазовое превращение сопровождается необратимым переходом в моноклинную систему, тогда как второй фазовый переход является обратимым. Температурная зависимость удельного электрического сопротивления показала аномалию при 712 К. Спектры отражения также указывают на образование новых фаз. Теллурит связан со слабым парамагнетизмом Паули. Кинетические параметры, вычисленные на основе ДСК данных, показали высокие значения энергии активации, энтропии активации и частотного множителя.